THE ASTROPHYSICAL JOURNAL, 467:851–859, 1996 August 20

SIMULTANEOUS MULTIWAVELENGTH OBSERVATIONS OF DWARF NOVAE. I. SU URSAE MAJORIS: MINIHUMPS AT A MINIOUTBURST?

J. ECHEVARRÍA,[1] G. TOVMASSIAN,[1,2] M. SHARA,[3] M. TAPIA,[1] J. BOHIGAS,[1] D. H. P. JONES,[4] R. GILMOZZI,[5] R. COSTERO,[6] J. A. LÓPEZ,[1] M. ROTH,[1,7] M. ALVAREZ,[1] L. F. RODRÍGUEZ,[6] E. DE LARA,[6] R. J. STOVER,[8] C. MARTINEZ-ROGER,[9] F. GARZÓN,[9] N. ASATRIAN,[2] N. VOGT,[10,11] P. SZKODY,[12] E. ZSOLDOS,[13] J. MATTEI,[14] AND F. M. BATESON[15]

Received 1995 May 24; accepted 1996 March 15

ABSTRACT

SU Ursae Majoris—the prototype of a subgroup of dwarf novae that display superhumps in superoutbursts has been observed during an international campaign dedicated to the observation of the first day of outburst of dwarf novae during 1986 February. After the start of a brightening was reported, the star was monitored by *IUE*, ground-based photometry and spectrophotometry, IR-photometry, and radio observations by VLA. However, it did not undergo a normal outburst or a superoutburst.

We observed a short and low-amplitude flare, consisting of two phases. The first phase lasted 22 hr, during which the system brightened in the UV and optical wavelengths by factors of 2 and 3.5, respectively; then, at long wavelengths it declined to its initial value, while in the UV the system remained at mid-brightness. In the second phase the system brightened again mainly at long wavelengths and reached half the intensity of the primary brightening. The spectral lines varied but remained in emission during the entire flare, which indicated that no transformation to the optically thick state occurred. The variations of fluxes of the UV emission lines are correlated with changes in the continuum, while the optical lines, observed with higher time resolution, show great variability in relative intensities and equivalent widths. The Balmer line ratios indicate higher densities and temperatures of the disk after the primary brightening, when a drop in luminosity at longer wavelengths was observed. Furthermore, multichannel photometry obtained during the first phase of the flare displayed coherent variations, probably modulated with half of the orbital period or several percent less. The study of the flux distribution during the flare confirmed that it is inconsistent with the simple steady state model of accretion disks, described by a single power law, probably because of the presence of a hot source contributing significantly around 2000 Å. The conclusion is drawn that the observed flare may be consistent with the mass transfer instability model of outburst of dwarf novae. The primary brightening could be interpreted as a burst of mass transfer striking the accretion disk. The enhanced bright spot gave rise to the light modulation. The consecutive drop and secondary brightening at long wavelengths could have resulted from the dissolution of the bright spot and disk shrinking due to the accretion of low angular momentum material into the disk and its successive restoration.

Subject headings: novae, cataclysmic variables — stars: individual (SU Ursae Majoris)

1. INTRODUCTION

Cataclysmic variables (CVs) are close binary systems with a white dwarf (WD) primary and a main-sequence late-type secondary overflowing its Roche lobe, transferring matter to the primary through an accretion disk. In the presence of a strong magnetic field in the WD, matter is transferred along the magnetic field lines. The SU Ursae Majoris stars are conspicuous for their superoutbursts, in which the emitted energy is about an order of magnitude greater than in a normal outburst. Superoutbursts occur less frequently than normal outbursts but are more predictable. During superoutbursts, a hump appears in the light curve shortly after maximum. These features are known as superhumps, and their period is a few percent in excess of the orbital period of the binary system. In addition to typical outbursts (which always last several days) some dwarf novae undergo

[1] Instituto de Astronomía, UNAM, Apdo. Post. 877, 22860, Ensenada, B.C., México; gag@bufadora.astrosen.unam.mx.
[2] Byurakan Astrophysical Observatory, 378433 Byurakan, Armenia.
[3] Space Telescope Science Institute, 3700 San Martin Drive, Baltimore, MD 21218; mshara@stsci.edu.
[4] Royal Greenwich Observatory, Madingley Road, Cambridge CB3 0EZ, UK; dhpj@ast.cam.ac.uk.
[5] *International Ultraviolet Explorer* Observatory, Villa Franca 54065, E-28080 Madrid, Spain; gilmozzi@stsci.edu.
[6] Instituto de Astronomía, UNAM, Apdo. Post. 70-264, 04510 México, D.F., México; costero@astroscu.unam.mx.
[7] Las Campanas Observatory, Casilla 601, La Serena, Chile; mroth@uchcecvm.bitnet.
[8] University of California Observatories/Lick Observatory, University of California, Santa Cruz, CA, 95064; richard@ucolick.org.
[9] Instituto de Astrofísica de Canarias, Vía Láctea, E-38200 La Laguna, Tenerife, Canary Islands, Spain; cmr@ll.iac.es, fgl@iac.es.
[10] Pontificia Universidad Católica de Chile, Astrophysics Group, Casilla 104, Santiago 22, Chile; vogt@nova.tat.physik.uni-tuebingen.de.
[11] Sternwarte Sonneberg, Sternwartenstr. 32 D-96515 Sonneberg, Germany.
[12] University of Washington, Seattle, WA 98195; szkody@alicar.astro.washington.edu.
[13] Konkoly Observatory, P.O. Box 67, H-1525 Budapest, Hungary.
[14] American Association of Variable Star Observers, 25 Birch Street, Cambridge, MA 02138; aavso@cfa0.harvard.edu.
[15] Royal Astronomical Society of New Zeland, PO Box 3093, Greerton, Tauranga, New Zealand.

"flares" with small amplitude (about 1–2 mag above quiescent level) and short duration (of the order of 12–48 hr). Bateson (1991a, 1991b, 1993) reports a total of 67 such flares in six southern dwarf novae, among them also the SU UMa stars OY Car, Z Cha, and TU Men. Often these flares occur as "precursors" 4–10 days before the next outburst.

An international campaign to observe dwarf novae (DNs) outbursts from the first day was held in 1986 February. The campaign covered the spectral range from UV to radio wavelengths. Ten sites around the world carried out different types of optical observations. The description of this campaign and very preliminary results were reported by Echevarría (1987). Six objects among 33 candidates were caught in the rise. Further results on those objects will be presented in a separate publication. The best wavelength and time coverage was obtained during a short and low-magnitude flare occurring in SU UMa. We avoid using the term "outburst" to refer to this event, since neither the amplitude nor the double-peaked 42 hr duration of the flare bear any resemblance to an outburst or superoutburst. However, it is too long-lasting and powerful to be considered as ordinary flickering. Recently, a similar low-amplitude, irregular flare in SU UMa was reported by Van Paradijs et al. (1994).

SU UMa, the prototype of the corresponding subclass of DN, is a low-inclination, noneclipsing close binary with an orbital period of 110 minutes (Thorstensen, Wade, & Oke 1986). In quiescence it usually flickers between magnitudes 15.0 and 14.2, rising to $m_V \simeq 12.2$ during outbursts and 11.2 at superoutburst. The mean outburst cycle is $\simeq 16$ days, while superoutbursts occur every 160 days (Ritter 1990). According to AAVSO (the American Assocation of Variable Star Observers), the previous outburst of SU UMa occurred 37 days before our observations. It lasted 5 days and had a 2 mag amplitude.

Although superhumps are one of the distinguishing properties of SU UMa type stars, these were discovered only recently in SU UMa (Udalski 1990). The period of the superhumps is 113.4 minutes, $\simeq 3\%$ longer than the orbital one. It was noticed that the superhump period decreased during the superoutburst, and two components, a compact and a broad source, were identified in the structure of the hump. These observations have been explained by the generally accepted model for superhumps, where the humps are produced by a precessing elliptical disk (Vogt 1981; Whitehurst 1988; Whitehurst & King 1991). This model, combined with thermal instabilities in the disk (Osaki 1989, Ichikawa, Hirosi, & Osaki 1993), yields a fair numerical simulation of a superoutburst.

Spectroscopy of SU UMa has been performed by a number of authors. It is included in the spectral survey of DNs by Oke & Wade (1982). Szkody (1981) reported that neither the power law describing the energy distribution of SU UMa, nor the He II $\lambda 1640$ and $\lambda 4686$ lines in the spectrum, are consistent with a steady state accretion model where $F_\lambda \sim \lambda^{-2.3}$, concluding that relative to other DNs the accretion disk of SU UMa is denser and hotter. Besides the orbital period of the system Thorstensen et al. (1986), discovered a possible pressure broadening in the Balmer lines, a difference in phases of the peaks versus the wings of emission lines, and the presence of Mg $\lambda 4481$ in the wing of He I. Voikhanskaya & Nazarenko (1985) found a partial inverse Balmer decrement, confirming that the accretion disk of SU UMa shortly after outburst is dense, and that there might be substantial density gradients within it. They also found deep narrow minima superposed on the radial velocity curve.

Ultraviolet observations of SU UMa during outburst have been carried out with the *ANS* (Wu & Panek 1983) and the *IUE* (Verbunt 1987), and the decline after outburst was observed by *IUE* (Woods, Drew, & Verbunt 1990). The *ANS* data showed SU UMa to have a very red precursor outburst 12 hr before it reached a blue maximum. The rise occurred in two steps, both of them very red. After the first maximum, the light curve declined to a level slightly above quiescence and then the light curve rose again. Moreover, from all these data it is obvious that the continuum shortward of 2000 Å and longward of 3000 Å vary differently. This leads to the conclusion that the optical and UV continua are produced in different regions.

2. OBSERVATIONS AND REDUCTION

2.1. *IUE Observations*

Ultraviolet spectra of SU UMa were obtained on February 8 and 9 by *IUE* at VILSPA and GSFC in the low-dispersion mode at both available spectral ranges, SWP and LWP, through a large aperture. The observation covered most of the flare. Exposure times varied according to the brightness of the system, usually exceeding half of the orbital period. A log of these observations is presented in Table 1.

The IUESIPS standard reduction package was applied to extract absolute flux and wavelength calibrated spectra at the *IUE* Data Analysis Center (RDAF). To reduce the SWP spectra we also used the NEWSIPS package (Nichols-Bohlin et al. 1993), which is more accurate and up to date. The differences between the two reduction procedures are not significant in this case. Further processing was done with IRAF. The continuum was measured at portions of spectra by averaging data in 15 Å wide bands, at which it was possible to avoid the influence of numerous emission lines. The continuum at the base of major lines was determined individually because of the complexity of the spectra and significant spectral variations of the continua during

TABLE 1

JOURNAL OF *IUE* OBSERVATIONS OF SU URSAE MAJORIS

Camera and Image ID	HJD Midexposure	Exposure Time (minutes)	FES (mag)
SWP 27682	2446469.95714	100	15.5
LWP 7639	2446469.99818	50	...
LWP 7640	2446470.30511	90	15.1
SWP 27684	2446470.36364	60	14.3
LWP 7641	2446470.41676	60	14.6
SWP 27685	2446470.56728	120	15.1
LWP 7642	2446470.66534	90	14.9
SWP 27686	2446470.77060	180	15.7
LWP 7643	2446470.85685	90	15.4
SWP 27687	2446470.95000	145	15.1
LWP 7644	2446471.03735	90	15.0
SWP 27688	2446471.12008	120	15.2
LWP 7645	2446471.20549	90	14.8
SWP 27689	2446471.27301	90	15.0
LWP 7646	2446471.33253	45	14.7
SWP 27690	2446471.39491	90	14.8
LWP 7647	2446471.45700	70	15.1
SWP 27691	2446471.58337	75	14.9
LWP 7648	2446471.63406	55	14.9
SWP 27692	2446471.68261	65	15.1

the observations. This may bring in systematic errors, which we tried to minimize by implementing different methods, so as to have some degree of confidence in the general behavior of the line parameters. Thus, the spread of values in the equivalent widths of the lines, depending on the chosen level of the continuum, may reach up to 10% overall. This value is somewhat higher than the rms value for a single line fitting.

2.2. *Optical Spectrophotometry*

Optical spectrophotometry of SU UMa's flare was obtained with a CCD detector attached to the Cassegrain spectrograph mounted at the Lick 1.0 m telescope, and with the UAGS spectrograph mounted on the Byurakan observatory 2.6 m telescope, using Kodak-103aO film and an image tube. The star was observed at Lick on February 8 with a spectral dispersion of 4.1 Å pixel^{-1} in the 4100–5800 Å range, on February 9 with a spectral dispersion of 2.75 Å pixel^{-1} in the 4600–5800 Å range, and February 10 with a dispersion of 8.0 Å pixel^{-1} in the 4200–7000 Å range. It was observed in Byurakan on February 8 from 3700–5400 Å with the 50 lines mm^{-1} dispersion mode. All dates are UT. The combined log of these observations is presented in Table 2.

Wavelength calibration at Lick suffered from new equipment installation problems. Thus, we used night sky lines (Osterbrock & Martel 1989) for wavelength calibration on February 8 when no calibration spectra was available. We used sky lines to adjust spectra on consecutive nights too, since calibration spectra display significant shifts from one exposure to another. An accuracy of 0.7 Å was reached.

The orbital phases were crudely estimated from measures of the center of Hβ by fitting a sine curve with the corresponding period provided by Thorstensen et al. (1986). The error in their period is too large to predict the phases of the present observations. Equivalent widths and absolute fluxes for Hβ and continuum in several regions were measured on Lick's higher resolution spectra on February 9. In addition to that, the measurement of other Balmer lines and He I λ4471 were available at pre- and postflare lower resolution spectra. Because the He I λ4921 line contaminates the red wing of Hβ, it was substracted after fitting a Gaussian using its red wing. At lower resolution the spectral deblending method provided by IRAF was used in order to measure very broad hydrogen lines.

At Byurakan a set of spectra was obtained when SU UMa was on the peak of the flare. The exposure times were chosen to fit a 12th magnitude star, but since the rise of SU UMa was not complete all spectra were underexposed. Nevertheless, two 240 s exposures were obtained and scanned with a PDS microdensitometer. Using comparison spectra, exposed on the same film, they were wavelength calibrated and scrunched. No absolute flux calibration was done because images overfilled the narrow slit, although they were normalized to the standard star energy distribution observed immediately after. The two spectra were added, so that time resolution was lost. Equivalent widths and relative fluxes of major lines were determined after evaluation of the continuum.

Measurements of emission lines from optical spectra obtained at Lick and Byurakan are presented in Table 4 below. Values of line parameters marked "after flare" and "secondary brightening" are means of several spectra obtained at corresponding periods. Measurement errors in the optical spectra are much less than in the UV, because of the better defined continuum and the higher S/N ratio. The statistical errors of our measurements are estimated to be within $\pm 2.5\%$.

TABLE 2

JOURNAL OF OPTICAL SPECTRAL OBSERVATIONS OF SU URSAE MAJORIS

Image ID	JD Start Exposure	Exposure Time (minutes)	FWHM Resolution (Å)	Spectral Region (Å)
		Lick 1.0 m Telescope		
01	2446469.8437	10	11	4100–5800
09	2446470.7299	10	7	4600–5800
10	2446470.7419	30	7	4600–5800
13	2446470.7778	30	7	4600–5800
15	2446470.8507	20	7	4600–5800
16	2446470.8674	20	7	4600–5800
19	2446470.8882	20	7	4600–5800
22	2446470.9240	20	7	4600–5800
23	2446470.9511	20	7	4600–5800
36	2446471.7778	20	20	4200–7000
37	2446471.8000	20	20	4200–7000
42	2446471.9174	20	20	4200–7000
		Byurakan 2.6 m Telescope		
07	2446470.4205	4	4	3650–4750
08	2446470.4209	4	4	4300–5400
11	2446470.4332	4	4	3650–4750
12	2446470.4337	4	4	4300–5400

2.3. *Optical and IR Photometry*

Optical photometry of SU UMa includes *UBVRI* observations with the 1 m Jacobus Kapteyn Telescope (JKT) at La Palma Observatory, and *JHK* photometry at the 1.5 m Carlos Sánchez Telescope (TCS) of the Instituto de Astrofísica de Canarias. The IR observations were made on February 8 and 10. The star was at the sensitivity limit of the IR photometer, and no variations were registered within a relatively large error. The corresponding magnitudes in *J*, *H*, and *K* were 14.0 ± 0.1, 14.5 ± 0.5, and 14.6 ± 0.8.

UBVRI photometry was done with a two-channel photometer with a "sky-star" scheme. The object and the sky were switched in the channels after each *UBVRI* sequence. Typical exposure times in each band were 10 s, while consecutive measurement with the same filter were done every 2 to 3 minutes. A comparison star was observed every half-hour or less. The primary peak was fully covered, and there are pre- and postflare measurements as well.

2.4. *VLA Radio Observations*

Radio continuum observations were made during the campaign with the VLA in the D/A configuration. Bandwidths of 50 MHz centered at 4885 and 4835 MHz were used simultaneously for on-source integration times of 10–40 minutes. The data were calibrated and edited following the standard VLA procedures. The highest possible S/N ratio was obtained by using natural weighting for data. No sources were detected among 11 DN systems in the areas mapped at the 4 σ levels. SU UMa was observed on several occasions and a map was made averaging all data. An upper limit of ≈ 0.15 mJy was obtained. This DN has been reported to have radio emission during ordinary outbursts (Benz, Furst, & Kiplinger 1983).

3. LIGHT CURVE

A light curve combining the V magnitudes from the optical photometry and fine error sensor (FES) magnitudes obtained by *IUE* is presented in Figure 1*a*.

The times at which the spectral observations were performed are marked at the bottom of the figure. The flare lasts for some 20 hr. A 1.2 mag increase is clearly seen in the light and a secondary, smoother brightening is also clear. Although the amplitude of the flare is comparable in amplitude to flickering, its duration and variations in the continuum and emission lines lead us to consider it as a unique event. In the following text we will refer to the peak at JD 2446470.4 as the "flare," while the term "after flare" will correspond to the drop of brightness at JD 2446470.75. Observations one day prior to the flare are referred to as "before flare," and observations the day after the flare, when the flux increased again, are referred to as "secondary brightening."

4. CONTINUUM

The continuum was traced from 1200 to 10000 Å. Light curves at different UV wavelengths are presented in the Figure 1*b*. Photometric light curves covering only the main peak of the flare will be discussed in § 6. Continuum in the *IUE* spectra was measured at four narrow (15 Å) bands shortward and longward of 1500 Å. This wavelength was selected because the continuum behaves differently on either side. The difference occurs mainly during the post-flare, where a steep drop of flux for $\lambda \geq 1500$ Å was observed, while the short-UV continuum stood at a constant level between the maximum and minimum values. Flux between 1200–1300 Å rose 2.15 times and fell by a factor of 1.8 within the following 5 hr. Around 2600 Å the corresponding numbers are 1.8 and 2.75 within 10 hr. In this spectral region, the decline is followed by a steady rise for the next 20 hr. Meanwhile, the short-wavelength part of the spectra remained in standstill, possibly declining toward the very end. The optical continuum during the flare and immediately after follows the LWP data. Unfortunately, the UV spectra were obtained with exposure times of the order of the intrinsic light variations and the orbital revolution, and cannot reveal rapid changes. Thus, the continuum obtained in SWP and LWP at different phases of the flare do not coincide very well. Also, line variations presented below were smoothed by rapid changes occurring during exposures. The FES and *UBVRI* data (Fig. 1*a*) show that the flare was very short-lived.

5. EMISSION LINES

The emission lines present in the spectra are common among DNs in quiescence. In Figure 2 the composite spectra of SU UMa at different times are presented.

The most important lines in the SWP spectra are N v λ1240, O i λ1305, C ii λ1335, Si iv λ1402, and particularly C iv λ1549, He ii λ1640, and Al iii λ1860. In the LWP spectra Mg ii is the most prominent line. In the optical, besides the usual Balmer series, several He i lines are present, as well as He ii λ4686. Traces of other weak emission features are identifiable. Line widths and intensities vary during the flare. The pattern of variations for C iv, Mg ii, and Hβ lines is presented in Figure 3.

Equivalent widths, intensities, and FWHM of the UV and optical lines at different phases of the flare are presented in Tables 3 and 4.

It is obvious that these emission lines were affected by the flare. Lines of higher excitation, originating at high-temperature regions (see C iv λ1549 in Fig. 3) seem to change more during the primary brightening, while Mg ii is sensitive to the brightness drop *after* the flare. The amplitude of variations is less in the UV than in the optical region. This might be owing to the relatively long exposures carried out in the UV. Nevertheless, the amplitude of variation of the UV lines exceeds 20%, more than the expected

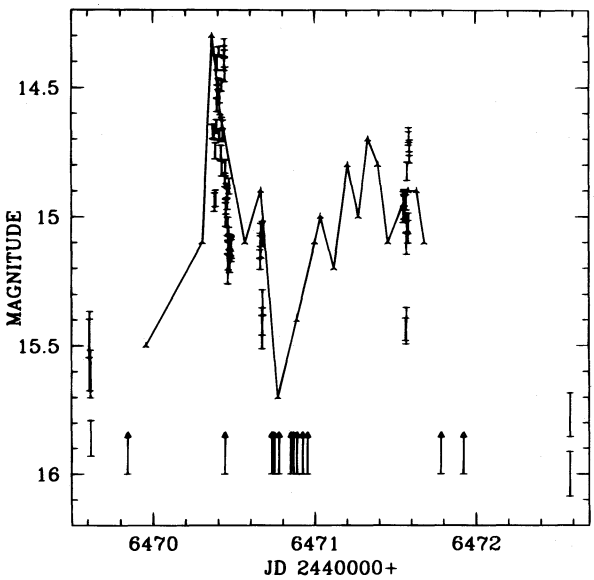

FIG. 1*a*

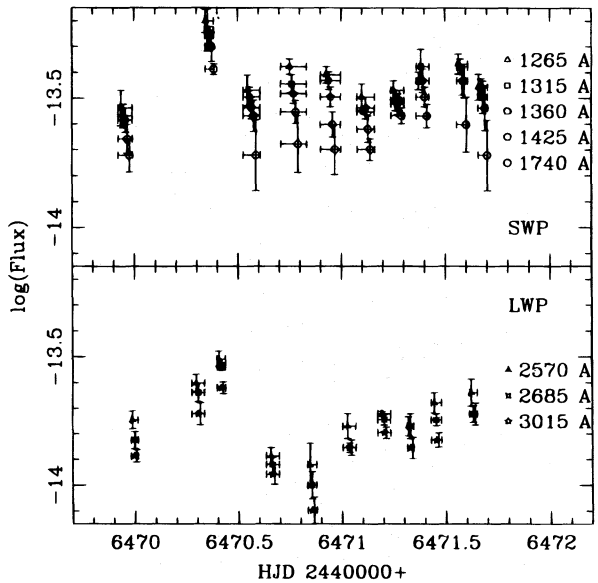

FIG. 1*b*

FIG. 1.—Light curve. (*a*) The line connects FES data, vertical bars indicate V magnitudes from *UBVRI* photometry. Dates when spectral observations were carried out are marked by arrows at the bottom of the figure. (*b*) The UV continuum, measured with 15 Å broad bandpasses centered at 1265, 1315, 1360, 1425, 1740, 2570, 2685, 3015 Å. Wavelength increases from top to bottom. Horizontal bars indicate exposure times. Vertical bars show accuracy of measurements. They are shifted from the center for better presentation.

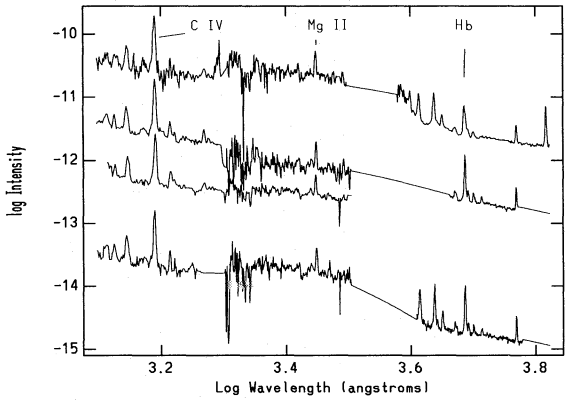

FIG. 2.—Composite spectra of SU UMa from *IUE* and optical observations. The first spectrum at the bottom corresponds to the quiescence *before* flare, next is the *flare* spectrum in the UV only, then *after* the flare, and finally at the top spectrum obtained at secondary brightening. The marks on the vertical axis are indicate log intensity relative to the first spectrum. The vertical scale for all consecutive spectra is shifted by one unit relative to each other.

TABLE 3

MEASUREMENTS OF ULTRAVIOLET LINE PARAMETERS

	Equivalent Width (Å)			Flux Ratio $F_\lambda/F_{C\,IV}$		
Emission Line	Before	Flare	After	Before	Flare	After
N v λ1240	−11.5	−13.7	−10.7	0.2	0.29	0.16
O i λ1305	−13.0	−15.0	−10.0	0.19	0.24	0.14
C ii λ1335.....	−9.0	−6.9	−7.5	0.14	0.12	0.1
Si iv λ1402.....	−25.0	−20.0	−24.0	0.29	0.35	0.3
C iv λ1549	−100	−68.9	−95.0	1.0	1.0	1.0
He ii λ1640	−14.0	−13.5	−15.0	0.13	0.16	0.12
Mg ii λ2800.....	−30.6	−21.3	−29.4	0.27	0.19	0.15

errors, which for the strong and distinct lines shown in Figure 3 should not exceed the 8%–10% level. Continuum fitting in the optical spectra was much easier and homogeneous, so that the errors are less than 5%. The main conclusions emerging from the optical spectrophotometry are as follows:

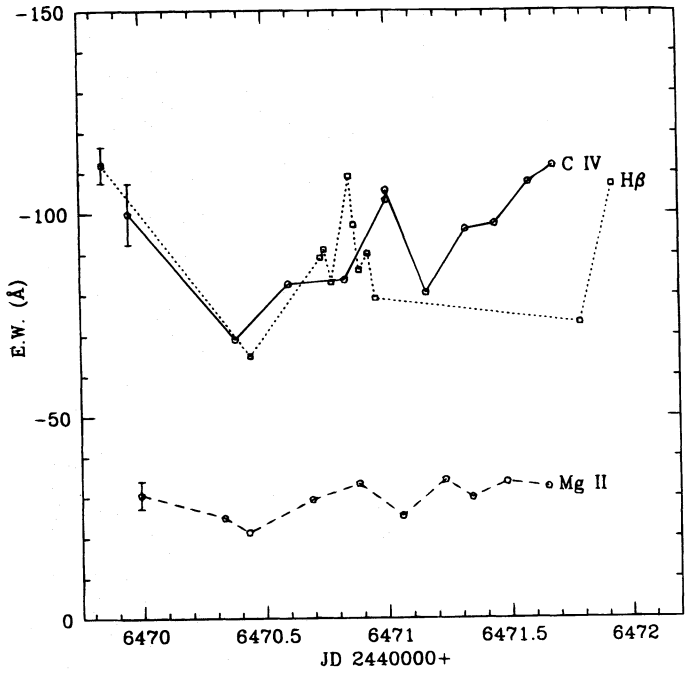

FIG. 3*a*

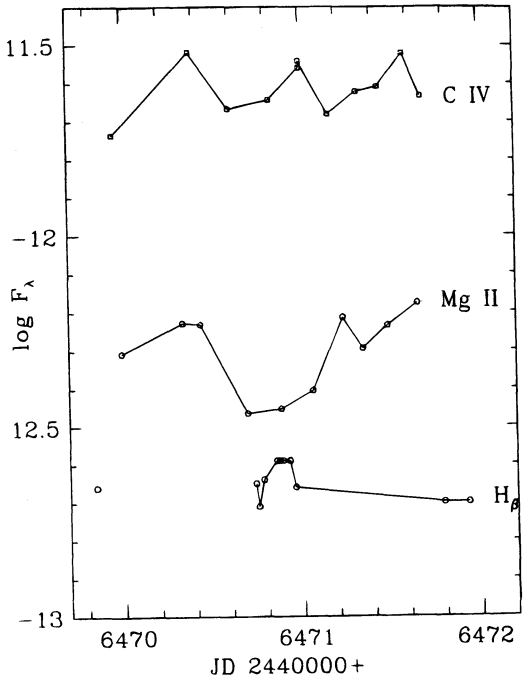

FIG. 3*b*

FIG. 3.—Variation of (*a*) equivalent widths and (*b*) total line fluxes of C iv, Mg ii, and Hβ during the flare. A typical error bar is shown for one point of each set.

TABLE 4

MEASUREMENTS OF OPTICAL LINE PARAMETERS

	Equivalent Width (Å)				Flux Ratio $F_\lambda/F_{H\beta}$				FWHM (Å)			
Emission Line	b	f	a	s.b.	b	f	a	s.b.	b	f	a	s.b.[a]
Hε.....	...	−7	...	...	...	0.27	...	...	...	17	...	...
Hδ	−65	−23	...	−53	0.83	0.4	...	0.88	27	22	...	33
Hγ.....	−97	−31	...	−97	0.87	0.63	...	1.29	22	20	...	33
He i λ4471	−33	−9	...	−31	0.28	0.18	...	0.4	29	10	...	44
He ii λ4868.....	−20	...	−25	−15	0.1	0.0	0.24	0.18	67	...	58	55
Hβ	−112	−65	−100	−90	1.0	1.0	1.0	1.0	24	21	25	43
Hα	...	...	...	−120	...	...	...	0.96	...	...	...	32

[a] "b" means *before*, "f" means *flare*, "a" means *after* and "s.b." means secondary brightening.

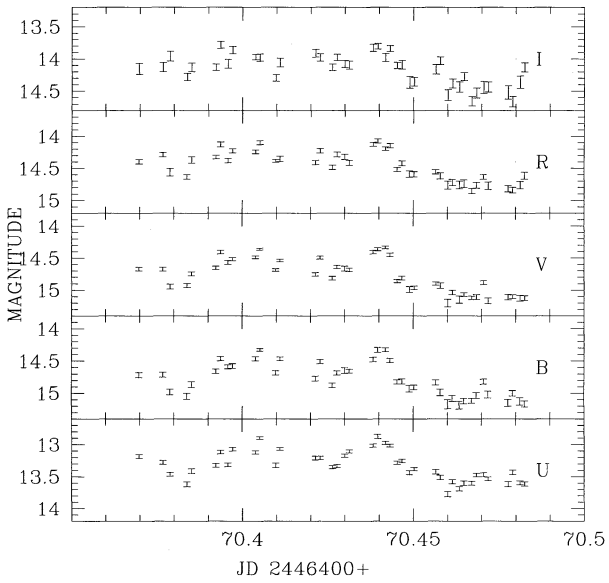

FIG. 4.—Light curves of SU UMa obtained from *UBVRI* photometry. The primary peak coverage is displayed. The markers length indicate measurement errors.

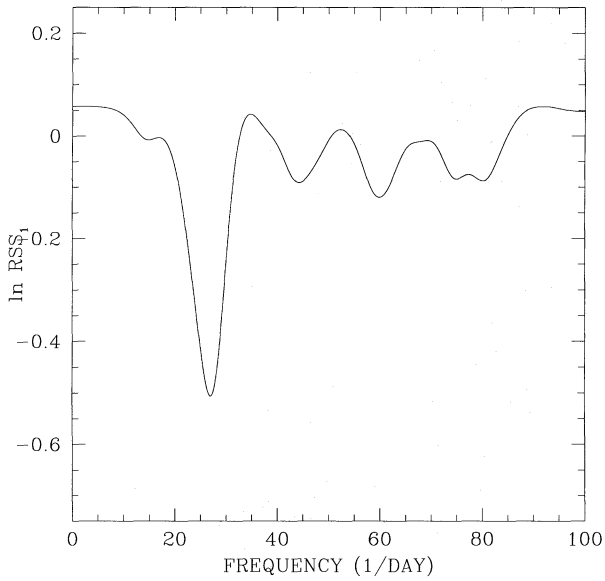

FIG. 6.—First-order residualgram. The combined *U* and *V* data were used to search for periods.

1. Balmer line ratios (i.e., Balmer decrement, see "Flux Ratio" column in Table 4) changed during observations, becoming partially inverted during *secondary brightening*, indicating very high temperatures and densities. Following Drake & Ulrich (1980), corresponding Balmer ratios lead to an electron density and temperature of 10^{12} cm^{-3} and 7000–9000 K in the flare, and $\geq 10^{14}$ cm^{-3} and 15,000–20,000 K during the *secondary brightening*. The appearance of a shoulder at $\approx$2300 Å at *secondary brightening* suggests the presence of a source at the corresponding temperature.

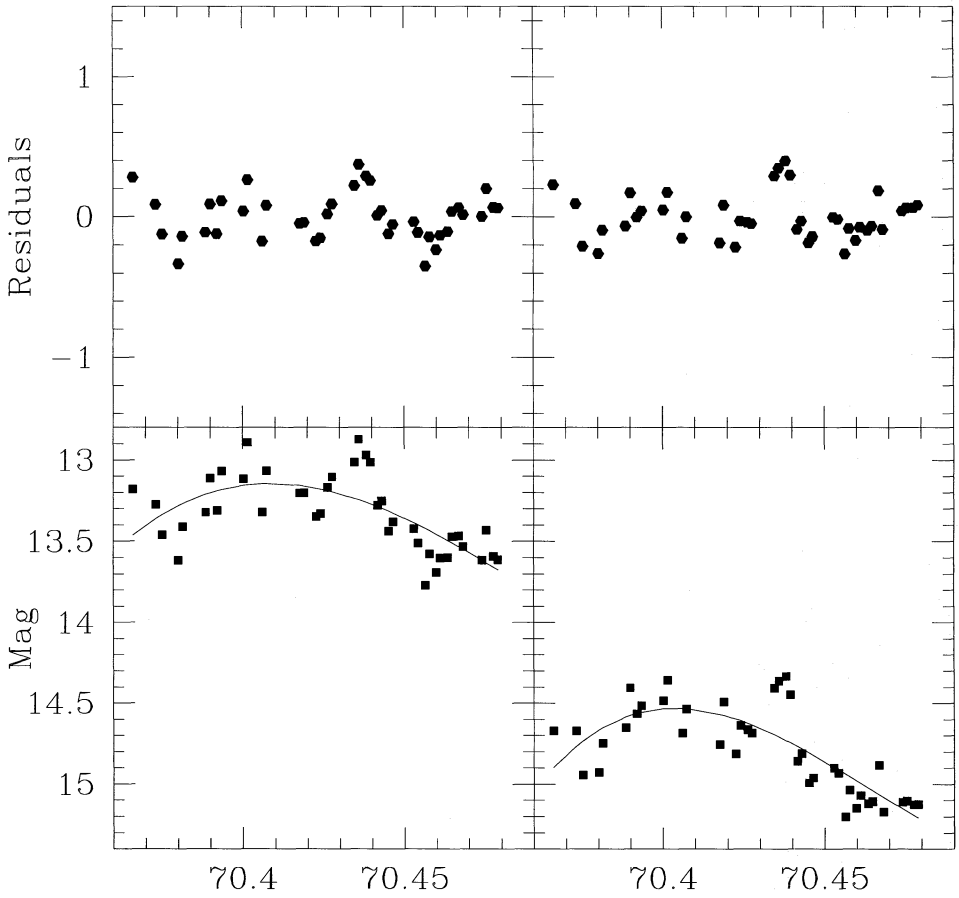

FIG. 5.—Least-square fits of flare by second-order polynomials and their residuals for *U* band on the left panel and *V* band on the right

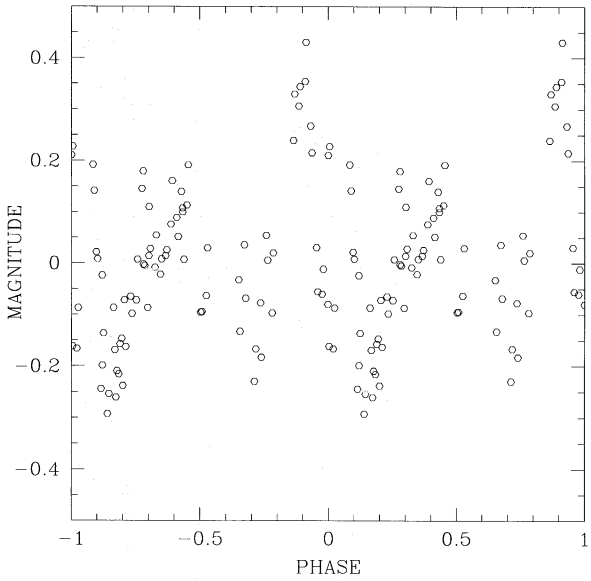

FIG. 7.—Same combined data folded on the superhump period obtained by Udalski. The *Y*-axis indicates the amplitude of variation in units of stellar magnitudes.

These estimates also are in agreement with the empirical data compiled by Echevarría (1987) and presented in a γ/β versus δ/β diagrams (see Figs. 1 and 11 in Echevarría 1987).

2. The FWHM of Hβ doubled from initially 20–25 Å to 40 Å after the flare. Although the latter was observed with lower spectral resolution, the other line widths observed on the same night with same equipment show that broadening is real. It might be caused by enhancement of the disk or the portion where emission lines are formed, or the presence of an additional component with a velocity different from that of the disk.

6. LIGHT MODULATIONS

A light curve from *UBVRI* photometry around the peak of the flare is presented in Figure 4. Mean errors for each band are displayed as vertical bars. The flare curve is superposed on a short-scale variability of smaller amplitude. These variations are quite normal in CV light curves and are known as flickering and/or quasi-periodic oscillations (QPO). However, the nature of both phenomena is not as yet clear.

The following procedure was applied to separate the short-scale variations from the flare curve. Light curves at the peak of the flare were adjusted with a second-order least-squares fit. These fits were subtracted from the observed data. The residuals (inverted) in the *U* and *V* bands are presented in Figure 5. They have approximately the same amplitude and are sparsely spread in time. To explore any possible periodic signal, residuals in both bands were combined in one file to increase time resolution. The *R*- and *I*-band data is relatively noisy. The addition of residuals in the *B* band was performed as well and did not have significant impact on the results presented here.

Since our data set is limited to one flare with a duration of a few hours, no certain results were anticipated. Nevertheless, we searched for periods close to the orbital and superhump periods and their first-order harmonics. The so-called period searching by least-squares method was applied to the data. This method is good enough for checking likely periods (Martinez & Koen 1994). The key to the method is to search for the minimum residuals between the set of observations and its least-squares fit by Fourier series. The resulting graph for the residuals for a range of periods from 15 to 180 mag is presented in Figure 6. The deepest minimum in the residualgram corresponds to $P = 0.03713$ day. This value is 2.8% less than half an orbital period. However, since the minimum is broad, we cannot determine if it corresponds to half an orbital period, half the superhump period, or if it is something new. The folding by phases add little to our knowledge: all resulting curves are as likely as not—depending on criteria. Nevertheless, we would like to draw attention to Figure 7, where the data are folded by a superhump period (not half!). This pattern can be identified with Udalski's (1990) two-component superhump shoulder with little effort. Therefore, it is possible that some light modulation during the flare, owing to inhomogeneities in the disk, was observed. The period of these modulations cannot be determined with any certainty from our observations.

7. ENERGY DISTRIBUTION

The energy distribution of SU UMa changed several times during the flare. The continuum distributions are plotted in an F_λ, log λ diagram in Figure 8. The energy distribution before the flare can be described by a λ^{-1} power law at short wavelengths, and a $\lambda^{-2.8}$ law beyond 2000 Å, far from the distribution expected for a steady state accretion disk. This distribution is also different from the one found by Szkody (1981), though it confirms that the UV and optical regions behave differently. Thus, either the sources producing the optical and UV emission are distinct and vary separately, or we see an additional source of radiation superposed on the normal flat flux distribution of the disk. At the peak of the flare the luminosity increases significantly more at both ends of the spectrum, and in particular in the *V* band, than in the spectral region around 2000 Å. We suspect that this can be partially accounted for by the fact that we missed the peak of the flare in the LWP exposure but not in the SWP. Yet other phases of the flare seem to confirm that there is a distinction between these spectral regions. Immediately after the peak, the luminosity decreases particularly at longer wavelengths, so that the resulting energy distribution *after* the flare is steeper, with a well-defined power law of $\lambda^{-2.33}$, though there still is apparent excess flux in LWP region. The continuum in the optical range was extracted from Lick spectra obtained at the corresponding time, since no *UBVRI* data were available. The continuum measurements in narrow bands free from lines from slit-spectrophotometry are systematically fainter than broadband *UBVRI* data. The secondary brightening occurs mainly at wavelengths longer than 1700 Å. The optical spectra obtained at this stage confirmed the steady flux rise at long wavelengths, when *IUE* had ceased observing.

However, the time resolution of *UBVRI* is much higher than of *IUE*; thus, three different distributions are presented reflecting highs and lows registered during *IUE* exposures. The points corresponding to optical spectra are presented too, though they were acquired later (see Fig. 1). The short end remains approximately constant, somewhat higher than the value *before* the main flare. The power law (-1.8), the blackbody (15,000 K) radiation curves, and their sum are shown on the same panel for comparison as a

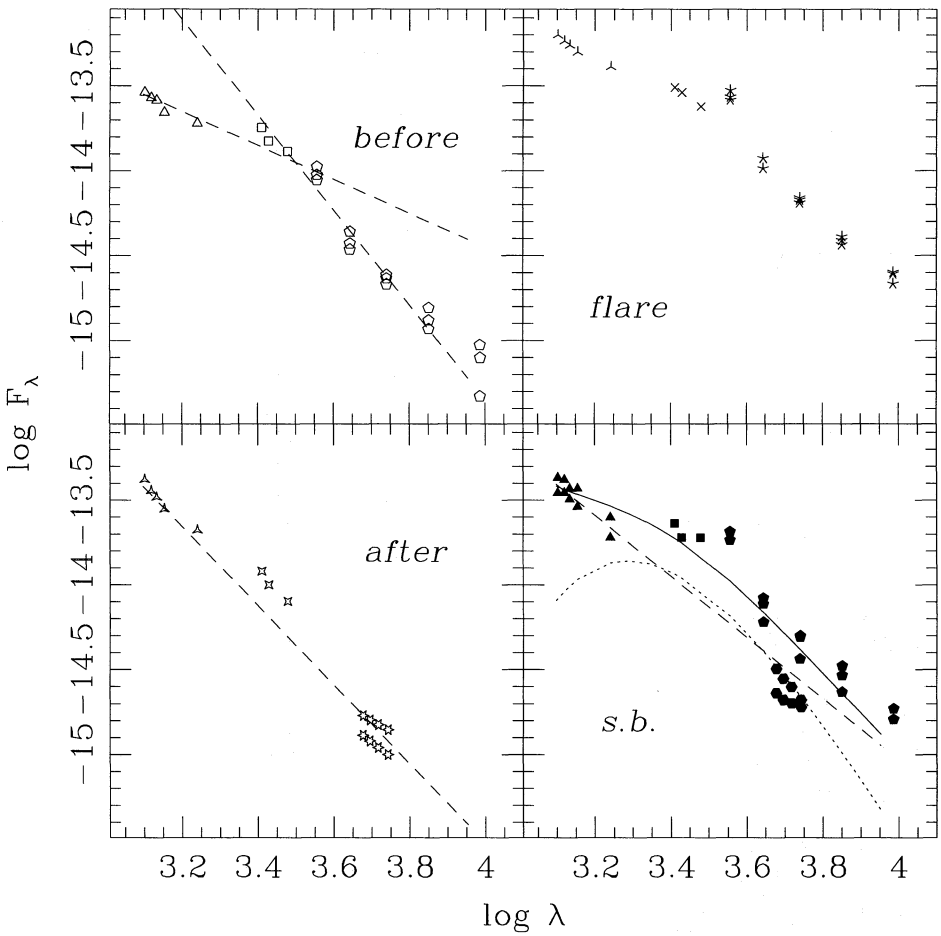

FIG. 8.—Flux distribution in different phases of the flare. On the top panels distribution *before* and at the flare are shown. On the bottom panels, figures indicate the distribution *after* the flare and during the secondary brightening. On all panels three-tip figures represent SWP data, four-tip figures represent LWP, five-tip figures represent *UBVRI* data, and six-tip presents continuum retrieved from optical spectra. In cases when several optical measurements were available during long *IUE* exposures, corresponding minimum and maximum are presented. The lines and curves present power-law and blackbody radiation. For indexes and description see text.

sample of possible two-component radiation. The curves on the figure are not fitted to empirical data and shifted by *Y*-axis to adjust for a better presentation.

The comparison of this flare with the ordinary outburst observed by Wu & Panek (1983) is very interesting. The light curves are double peaked in both cases, and the flux distribution *before* both events, as well as the duration of primary brightening and decline, are remarkably similar. However, the flux distribution evaluations run in opposite directions. In this minor outburst, which we called a flare, there is a steeper increase in the far UV than in the mid-UV, and the decline is more pronounced in mid-UV and longer wavelengths. Wu & Panek (1983) found a very red initial peak followed by a decline to an intermediate level, also with red flux distribution. Then, the flux at 1550–2200 Å recovered to the level reached at the initial peak, whereas the flux at 2500–3300 Å remained at an intermediate level. The secondary brightening led to the optical outburst peak at a 12.0 mag level, while in our observation the outburst did not occur.

8. DISCUSSION

The aim of the program under which the flare of SU UMa was observed was to determine the most likely outburst mechanism, either the disk instability model (Osaki 1974; Bath & Pringle 1982) or the mass transfer instability model (Bath 1973; Bath et al. 1974). The best way to determine which is the most likely, is to observe the outburst from its beginning. Though in the case of SU UMa we failed to observe an ordinary outburst or a superoutburst, we still obtained some valuable information, if we assume that the observed event was a disrupted preoutburst.

Briefly, the essence of the disk instability model is that periods of comparatively low accretion onto the WD, during which matter infalling from the secondary is accumulated in the outer disk, alternate with events of enhanced accretion triggered by instability in the disk owing to an enhanced viscosity parameter. The latter is thought to depend on the surface density of the disk, which varies because of the ionization of hydrogen. According to Papaloizou, Faulkner, & Lin (1983), the outburst can start in different regions of the disk. A change in the ionization state can start from the innermost disk, if during quiescence the entire disk is optically thin and cool and viscosity is large enough for the inner regions to become optically thick first. The increased temperature will heat the outer parts, forming an ionization wave directed outward. If the disk viscosity is small, the ionization process will start at the intermediate regions and will form two waves, one traveling outward and the other traveling inward. If considerable parts of the inner disk are already ionized, the outburst will

occur in the outer part only. This outburst can be interrupted in the second case, if not all of the outer disk is fully ionized as the outburst develops. In such an instance, a cooling front originates at the outer interface between the hot and cool areas and moves inward to quench the outburst. In every instance it is assumed that a sufficiently large fraction of the disk becomes optically thick, causing the depression of emission lines until wide absorption features develop. Our observations of SU UMa cannot be accounted for by this model, since the conversion of the entire disk into the optically thick regime was never seen.

In the mass transfer model the outburst is thought to be caused by a sudden mass transfer enhancement from the secondary into the disk. It stops when there is not sufficient energy to lift further material to the Roche surface. Since very little is known about the atmospheres of secondary stars in CVs, the mass burst profile is a free parameter, and a large variety of light curves can be produced. What is remarkable in the transfer instability model (Bath & Pringle 1981) is the prediction that the disk shrinks at the initial phase of the outburst, since matter accreted as a result of the instability in the secondary has a small angular momentum. The model also predicts the formation of an intense bright spot with a luminosity comparable to that of the disk. The timescale of preoutburst transitions is of the order of 10^5 s. These transitions may have been observed in the SU UMa flare. The pulse-shaped primary peak can be interpreted as the impact of the burst of matter into the disk. The brief modulations of light at the peak could be caused by the powered bright spot. The steep decrease of luminosity at long wavelengths might result from the dissolution of the bright spot and collapse of the outer cooler parts of the disk. At this stage we observed a pure accretion disk, but at lower luminosity. Since there was not enough heating it did not become optically thick, which would be evinced by the conversion to an absorption spectrum, and did not lead to an ordinary outburst. It is possible also that mass transfer instabilities generally do not lead to outbursts, which could not be proven or denied from this single event. The secondary brightening might have been produced by the restoration of mass transfer and a bright spot. It could cause a broadening of emission lines in the postoutburst spectra.

9. SUMMARY

We observed SU Ursae Majoris during an unusual small-magnitude, short-lasting outburst. Observations include ultraviolet and optical spectroscopy, optical photometry, and infrared and radio observations.

For $\lambda \gtrsim 1500$ Å the star undergoes a rapid flare with a 1.3 mag amplitude, lasting ≈ 1 day. Then it fades to its initial level and has a second brightening. Spectroscopic observations during this phase show nonsymmetrical Balmer line profiles. The Balmer line ratios are inverted during this phase. Optical photometry revealed rapid, possibly periodic, variations imposed on the light curve of the flare. Short of 1500 Å the star levels out at an intermediate magnitude.

The observed data allow us to suspect that there was a sudden burst in the mass transfer rate of the binary system. The presence of periodic light variations in the light curve assumes that the source is not the entire disk, but rather part of it, maybe a hot spot. Altogether, we interpret this event as an enhanced inflow of matter from the secondary to the disk. It generates the flare and creates a brighter hot spot. Then the mass transfer reduces to the previous rate or even less. The outer (cooler) parts of the accretion disk shrink since the inflow brings low angular momentum material into it. As a result, the luminosity abruptly decreases.

We would like to thank the staff in the different observatories for their kind support. We are especially grateful to W. Wamsteker and Y. Kondo for their generous help with *IUE* facilities. Special thanks to J. Barral and R. Michel for helping in the observations.

REFERENCES

Bateson, F. M. 1991a, Publ. Variable Star Sec. R. Astron. Soc. New Zealand, 16, 75
———. 1991b, Publ. Variable Star Sec. R. Astron. Soc. New Zealand, 17, 74
———. 1993, Publ. Variable Star Sec. R. Astron. Soc. New Zealand, 19, 54
Bath, G. T. 1973, Nature Phys. Sci., 246, 84
Bath, G. T., Evans, W. D., Papaloizou, J., & Pringle, J. E. 1974, MNRAS, 169, 447
Bath, G. T., & Pringle, J. E. 1981, MNRAS, 194, 967
———. 1982, MNRAS, 199, 267
Benz, A. O., Furst, E., & Kiplinger, A. L. 1983, Nature, 305, 36
Cordova F. A., & Mason K. O. 1983, in Accretion Driven Stellar X-Ray Sources, ed. W. H. G. Lewin & E. D. J. van der Heuvel (Cambridge: Cambridge Univ. Press), 147
Drake, S. A., & Ulrich, R. K. 1980, ApJS, 42, 351
Echevarría, J. 1987, Ap&SS, 130, 103
Ichikawa, S., Hirose, M., & Osaki, Y. 1993, PASJ, 45, 243
Lynden-Bell, D. 1969, Nature, 223, 690
Martinez, P., & Koen, C. 1994, MNRAS, 267, 1039
Nicholas-Bohlin, J. S., Garhart, M. P., De La Peña, M. D., & Levay, K. L. 1993, *IUE* NASA Newsletter, 53, 1
Oke, J. B., & Wade R. A. 1982, AJ, 87, 670
Osaki, Y. 1974, PASJ, 26, 429
———. 1989, PASJ, 41, 1005
Osterbrock, D. E., & Martel, A. 1989, UCO/LO Bulletin No. 1205
Papaloizou, J., Faulkner, J., & Lin, D. N. C. 1983, MNRAS, 205, 487
Ritter, H. 1990, A&AS, 85, 1179
Shakura, N. I., & Syunyev, R. A. 1973, A&A, 24, 337
Szkody, P. 1981, ApJ, 247, 577
Szkody, P., & Cropper, M. 1988, in Multiwavelength Astrophysics, ed. F. Cordova (Cambridge: Cambridge Univ. Press), 109
Thorstensen, J. R., Wade, R. A., & Oke, J. B. 1986, ApJ, 309, 721
Tylenda, R. 1977, Acta Astron., 27, 235
Udalski, A. 1990, AJ, 100, 226
van Paradijs, J., et al. 1994, MNRAS, 267, 465
Verbunt, F. 1987, A&AS, 71, 339
Vogt, N. 1981, ApJ, 252, 653
Voikhanskaya, N. F., & Nazarenko, I. I. 1985, Soviet Astron., 62, 81
Whitehurst, R. 1988, MNRAS, 232, 35
Whitehurst, R., & King, A. 1991, MNRAS, 249, 25
Woods, J. A., Drew, J. E., & Verbunt, F. 1990, MNRAS, 245, 323
Wu, C. C., & Panek, R. J. 1983, ApJ, 271, 754